ELSEVIER

Coordination Chemistry Reviews
185–186 (1999) 37–51

COORDINATION CHEMISTRY REVIEWS

Ring slippage in indenyl complexes: structure and bonding☆

Maria José Calhorda [a,b,*], Luís F. Veiros [c]

[a] *Departamento Química e Bioquímica, Faculdade de Ciências, Universidade de Lisboa, Campo Grande, 1749-016 Lisbon, Portugal*
[b] *ITQB, Quinta do Marqués, EAN, Apart, 127, 2781-901 Oeiras, Portugal*
[c] *CQE, Instituto Superior Técnico, Av. Rovisco Pais, 1049-001 Lisbon, Portugal*

Received 6 August 1998

Contents

Abstract

A review of some structural and reactivity aspects of the coordinated indenyl ligand, dealing mainly with the systems theoretically studied by the authors is presented. In the first section, the structural characterization of η^5 and η^3 indenyl is attempted, noticing that the nodal properties of the π orbitals of the indenyl prevent a totally symmetric coordination in a η^5-indenyl. The two bonds to the hinge carbon atoms are always longer, and the distance becomes longer than a M–C bond in the η^3-indenyl derivatives. Some intermediate distances

☆ Dedicated to Professor Carlos C. Romão on the occasion of his 50th birthday.

* Corresponding author. Correspondence address: ITQB, Quinta do Marquês, EAN, Apart. 127, 2781-901 Oeiras, Portugal. Tel.: +351-1-4469451; fax: +351-1-4411277.
E-mail address: mjc@itqb.unl.pt (M.J. Calhorda)

PII: S0010-8545(98)00247-1

are found in [$(Ind)_2Ni$] where, formally, the ligand is halfway between η^5 and η^3. The ring slippage occurs when two electrons are added to the system, occupying a metal–indenyl antibonding orbital, which becomes more stable upon folding. We reviewed electrochemical and ligand addition driven slippage, in the second section. A comparison with the behavior of the cyclopentadienyl ligand was attempted in the end.

Keywords: Indenyl slippage; Haptotropic shift; Molecular orbital calculations

1. Introduction

Polienyl ligands can undergo haptotropic shifts, thereby changing the electron count around a metal center. The ease of this process can be related to the rate of some reactions, namely substitution reactions, which are significantly accelerated when a cyclopentadienyl ligand (Cp) is replaced by an indenyl (Ind)—the indenyl effect. Basolo introduced this term and described this mechanism of indenyl slippage [1]. The possibility of such occurrence during reactions is backed by the knowledge of several coordination modes exhibited by the polienyl ligands in a wide range of structurally characterized complexes which can be traced using the Cambridge Crystallographic Data Base [2]. As a matter of fact, a pure η^5 coordination, with five equivalent M–C bonds, is never observed, a slightly distorted $\eta^3 + \eta^2$ mode, where two bonds are slightly longer, being the rule, as will be discussed below.

Many studies, both experimental and theoretical, have been dedicated to understanding the indenyl effect and the factors which govern indenyl slippage. The addition of two electrons has been shown to induce a $\eta^5 \rightarrow \eta^3$ shift in systems such as [$(\eta^5$-Ind$)_2(CO)_2V$] [3], [$(\eta^5$-Ind$)CpMoL_2]^{2+}$ [4], [$(\eta^5$-Ind$)(CO)_3Mn$] [5], [$(\eta^5$-Ind$)(\eta^4$-cod$)Rh$] [6], and parallels in some way which also happens for the $\eta^6 \rightarrow \eta^4$ shift in arene complexes [7]. In the [$(\eta^5$-Ind$)CpMoL_2]^{2+}$ system, the η^5-Ind complex and the two-electron reduction product, a η^3-Ind species, were, for the first time, both structurally characterized for $L = P(OMe)_3$ ([4]b–d). On the other hand, the η^3-indenyl derivative was detected or postulated as an intermediate in several substitution reactions [8] and the possibility of occurrence of the indenyl effect was anticipated in designing a specific catalytic hydroboration reaction [9]. Indenyl slippage can also be induced by the addition of a ligand, an alternative way of adding two electrons to the metal center, as was observed for [$(\eta^5$-Ind$)Mo(CO)_2L_2]^+$ complexes for some L ligands and an entering nitrile, but did not take place for other ligands or entering groups [10]. In view of the interest awakened by this peculiar reactivity of the coordinated indenyl ring, it is not surprising that patterns typical of η^5-Ind and η^3-Ind coordination have been searched. Structural aspects were perhaps those analyzed in more detail [11], but the use of NMR to detect the hapticipty of indenyl in solution is also extremely important [12].

Some theoretical studies were done, based on extended Hückel calculations, in order to explain the bonding mode of the indenyl ligand in its possible hapticities [13] and to understand the indenyl effect [14].

In this work, we shall review the bonding and structural features, as well as some reactivity aspects, in some families of indenyl complexes, based on our recent work ([4]b, [10]), and compare our findings with some other literature results. The theoretical calculations supporting our reasoning are of the extended Hückel [15] and dft [16] type.

2. Results and discussion

2.1. Structural features of η^5-indenyl and η^3-indenyl coordination and theoretical interpretation

As mentioned above, the indenyl ligand can coordinate, in principle, in a perfect η^5 mode, where all the five M–C bonds have the same length, and in a slightly distorted so-called $\eta^3+\eta^2$ way, where the two M–C bonds to the hinge carbon atoms (4, 9) are longer than the other three M–C bonds (to 1, 2, 3), as depicted in Scheme 1. The η^3 and η^1 coordination modes are also represented.

Among the available structures [2], [(η^5-Ind)$_2$Fe] has been considered as an example of nearly perfect η^5 coordination [17], but a closer look at the metal–carbon distances clearly shows that two of them are longer [2.047(3), 2.041(3), and 2.049(4) vs. 2.101(4), 2.094(4) Å]. Indeed, the nodal character of the indenyl π orbitals (Scheme 2), introducing an asymmetry not present in the cyclopentadienyl orbitals, owing to the fact that the hinge carbons do not contribute to all of them (see $2\pi_s$, for instance; the notation of Ref. [14] is used), is responsible for this feature.

Extended Hückel calculations performed on an idealized model of C_{2v} symmetry of [(η^5-Ind)$_2$Fe] (Fe–C distance 2.08 Å) led to overlap populations of 0.145 (Fe–C2), 0.158 (Fe–C1,3), and 0.107 (Fe–C4,9), suggesting that the two Fe–C bonds to the hinge carbon atoms should indeed be weaker, as observed.

Faller et al. introduced several parameters to characterize the coordination of the indenyl ring [11]. As just described, there is no such thing as a perfect η^5 coordination, so that we shall consider as η^5 coordination the $\eta^3+\eta^2$ mode. Typical distances, as found in [(η^5-Ind)CpMo{P(OMe)$_3$}$_2$][BF$_4$]$_2$, are 2.276(7),

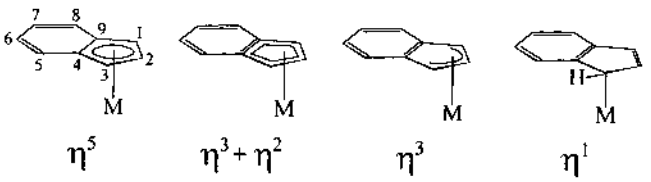

Scheme 1.

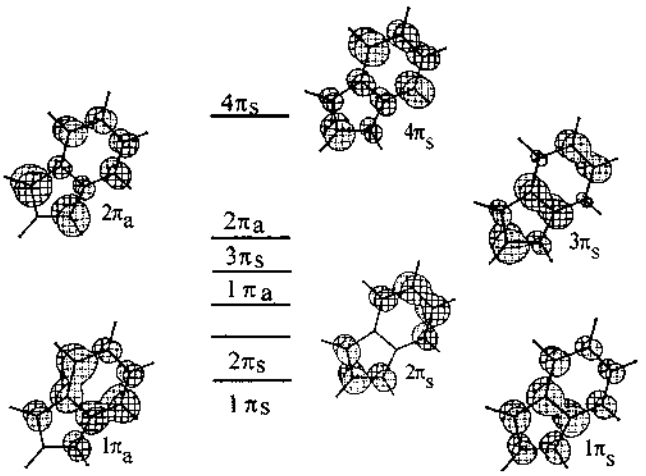

Scheme 2.

2.287(6), 2.309(5), 2.429(5) and 2.453(5) Å ([4]b, d), where the divergence between the two sets of distances is larger than what was found for $[(\eta^5\text{-Ind})_2Fe]$.

As the distortion away from perfect η^5 coordination increases, there is a slip of the metal relative to the center of the pentagon, a parameter used by Mingos to quantify the slip distortion in the carborane complexes [18]. A significant difference is that in the carboranes the pentagon remains planar, while in the indenyl it folds, so that the parameter becomes much less useful. On the other hand, the fold angle (angle between the plane of carbon atoms 1, 2, 3 and carbon atoms 1, 3, 4, 9, in Scheme 1) increases with the slip and is a more comfortable parameter. For our purposes, we can have a reliable description of the coordination model, on structural grounds, using only the M–C distances and the fold angle. This angle is close to 0° for η^5 coordination. In the complex $[(\eta^5\text{-Ind})CpMo\{P(OMe)_3\}_2][BF_4]_2$ the value is 4.1°. On the other hand, in a typical η^3-coordinated ligand, the fold angle is considerably higher. For instance, in $[(\eta^3\text{-Ind})CpMo\{P(OMe)_3\}_2]$ ([4]b), it is 21.7°, and the three Mo–C bonds 2.209(5), 2.359(6) and 2.362(6) Å. The Mo–C4, C9 distances are, respectively, 3.029(6) and 3.039(6) Å, outside bonding range, but useful for comparison.

The next aspect which is very interesting, but was not yet very apparent at the time Faller et al. published their work [11], concerns the relative orientation of the indenyl and the other ligands. Their thumb's rule applies to many η^5 compounds, but is not obeyed in many examples, such as the iridium derivative $[(\eta^3\text{-Ind})IrH_2(P^iPr_3)_2]$ [19].

In a previous work, we studied in detail the structural preferences of two groups of complexes which interconvert by addition of a nitrile, forcing the η^5-indenyl to become η^3-indenyl [10]. The two compounds involved are $[(\eta^5\text{-Ind})Mo(CO)_2(NCMe)_2]^+$ and $[(\eta^3\text{-Ind})Mo(CO)_2(NCMe)_3]^+$, the methyl being replaced by H in the dft calculations. In Fig. 1, we show the two limiting geometries

for both complexes and their relative energies, calculated with the Amsterdam Density Functional (ADF) program [20].

In the η^5-indenyl complex, the benzene ring lies opposite the carbonyl ligands as expected [11] and the energy difference is larger than for the other complex, where a 180° rotation of the ring took place. These results reflect the features of the experimentally determined structures [10,21]. It is easier to rationalize the behavior in the η^3 case, as the pattern is more clearly cut and the argument applies qualitatively, to our knowledge, in all the situations we tested. For this purpose, we use a molecular orbital diagram, taken from extended Hückel calculations, which is shown in Fig. 2.

A similar diagram is discussed in detail in [10], and the benzene ring lies over the carbonyl groups because this conformation maximizes backdonation to them, keeping a relatively strong bond between the indenyl and the metal. This effect can be clearly traced to the highest occupied molecular orbital (HOMO) as shown in Fig. 3.

When nitriles are substituted by bulkier groups, such as phosphines, this conformation becomes impossible for steric reasons. Indeed, no phosphine complexes of the kind $[(\eta^3\text{-Ind})Mo(CO)_2(PR_3)_2(NCMe)]^+$ are known. For a ligand of similar size, the conclusions hold.

The second family of compounds to be analyzed includes $[(\eta^5\text{-Ind})CpMoL_2]^{2+}$ and $[(\eta^3\text{-Ind})CpMoL_2]$ [4], and the ligands are exactly the same in both. Only the electron count changes. In the previous case, there was an extra ligand in the η^3-Ind complex, as the indenyl change in hapticity was induced by addition of this extra ligand. Again, the orientation of the indenyl relative to the L ligands differs, as can

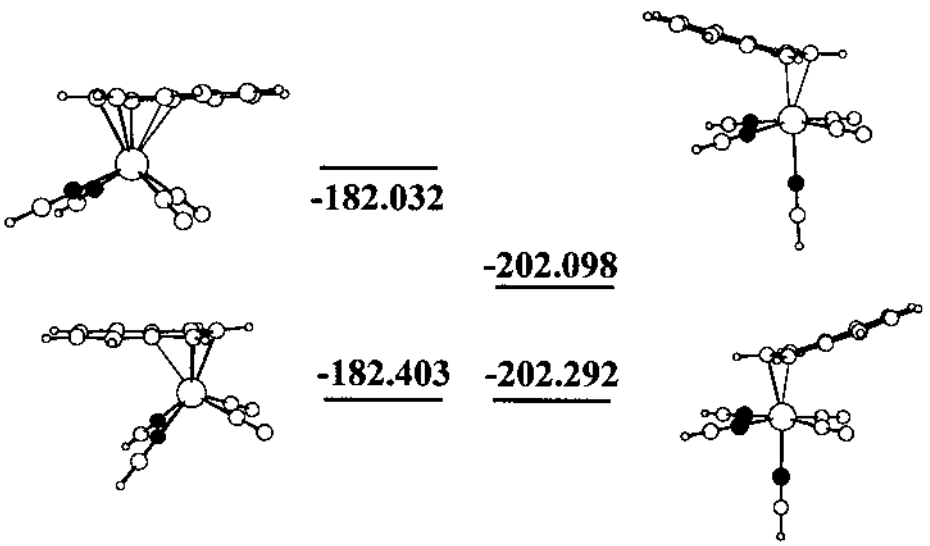

Fig. 1. Relative energies (eV) for the two limiting geometries of the cations $[(\eta^5\text{-Ind})Mo(CO)_2(NCH)_2]^+$ (left) and $[(\eta^3\text{-Ind})Mo(CO)_2(NCH)_3]^+$ (right). ●, indicates the nitrogen atoms.

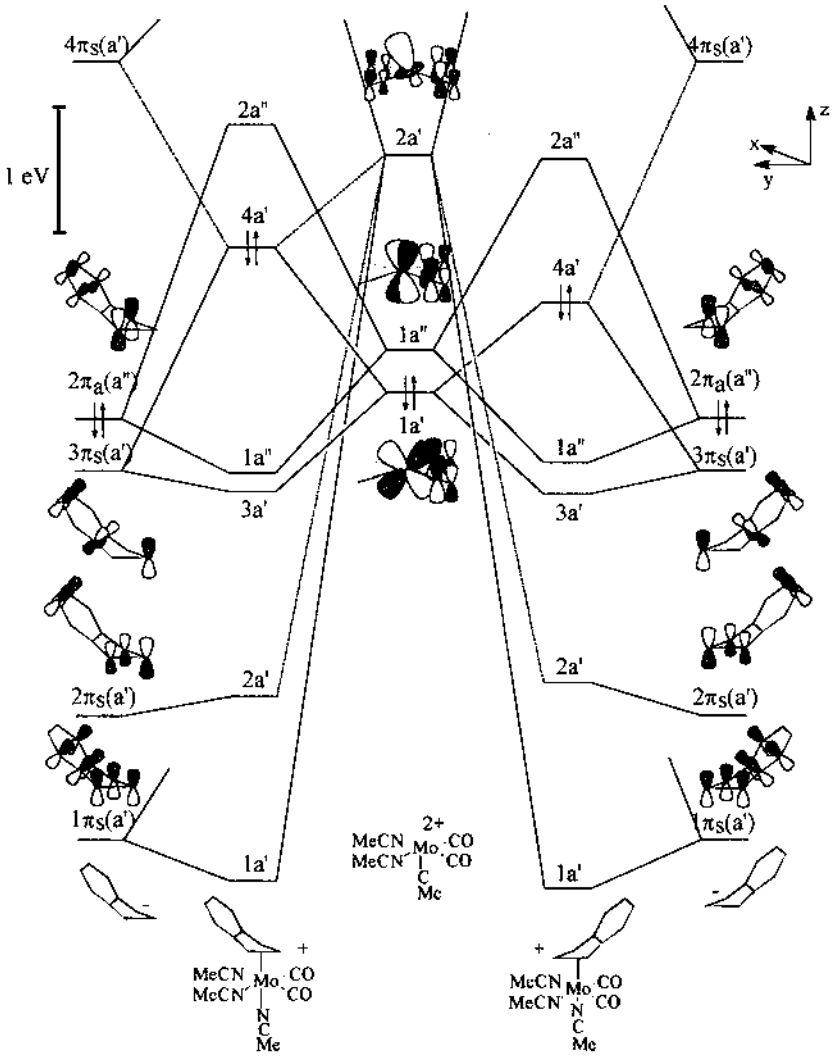

Fig. 2. Molecular orbital diagram showing the interaction between $[(CO)_2(NCMe)_3Mo]^{2+}$ fragment and the η^3-indenyl ligand in the less stable conformation (left) or the most stable conformation (right).

be seen in the dft optimized geometry for each of them, shown in Scheme 3. These orientations agree with the structural features determined by X-ray diffraction.

In this case, the origin of the preference is steric, as the η^3-indenyl may eclipse the Cp, but the η^5-indenyl, being almost planar and without a significant slip distortion, may not. It rotates ca. 90° to avoid steric repulsion. Such arrangements are found in many similar complexes [2].

We analyze now the family $[(Ind)_2M]$ (M = Fe, Co, Ni) ([13]b, [17]), where the iron derivative is an 18-electron complex, the cobalt derivative has one extra

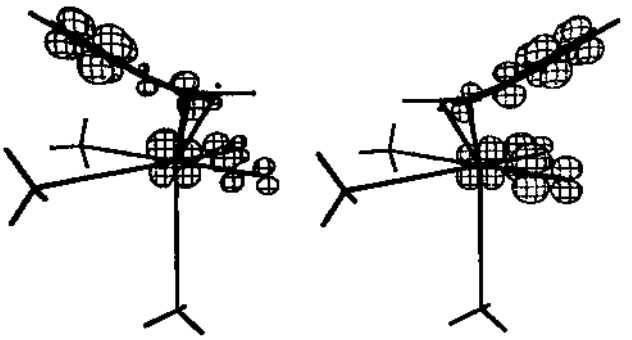

Fig. 3. The HOMO of $[(\eta^3\text{-Ind})Mo(CO)_2(NCMe)_3]^+$ in the two opposite indenyl conformations: the less stable (left) and the more stable (right).

electron (19 electron) and the nickel is formally a 20-electron compound. Their structures also differ. As described above, $[(\eta^5\text{-Ind})_2Fe]$ resembles, as much as possible, a complex of the perfect η^5-indenyl, the two rings being eclipsed. The energy of the staggered conformation differs only by 0.04 eV. As one moves to cobalt, there is some distortion in the metal coordination sphere, but the rings maintain the same conformation. Finally, for Ni, the two rings are staggered (this conformation has now become 0.2 eV more stable, still according to EH calculations), a side view of the structure shows to the naked eye an indenyl which looks η^3, and the slip is obvious. The Ni–C bonds are 1.973(3), 2.068(3), 2.056(3), 2.480(3) and 2.483(3). The asymmetry is plain, but is not enough to describe a true η^3-indenyl, as the authors state [17]. $[(Ind)_2Ni]$ therefore avoids being a 20-electron species, but two η^3-indenyl rings would make it a 16-electron compound. Indeed, if we count electrons, the complex has two extra electrons relative to iron, so that each indenyl has one extra electron relative to a η^5-indenyl, but is one electron behind relative to a η^3-indenyl. The coordination geometry of this indenyl is particularly interesting to compare indenyl complexes half-way through their 2e oxidation or reduction pathway, which are not isolable in many cases.

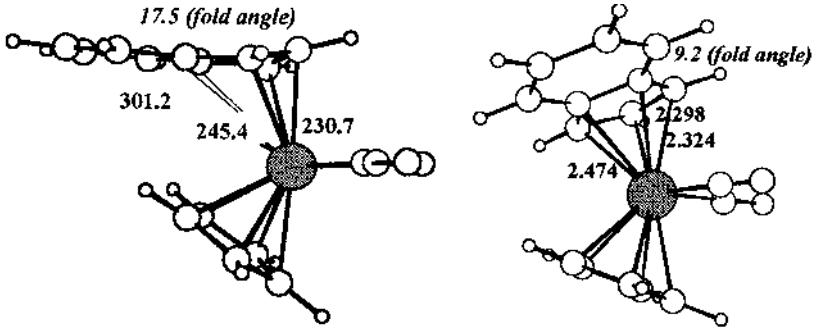

Scheme 3.

Scheme 4.

Concerning the relative arrangement of the indenyl rings, the Fe derivative is an analogue of eclipsed ferrocene, and the cobalt complex is very similar. Why is there a change in the nickel species? We performed extended Hückel calculations using the real structure. As will be discussed in more detail in the next section, when two electrons are added to a η^5-indenyl complex, they occupy a metal–indenyl antibonding orbital. The antibonding character decreases upon bending the ring and a breaking of the symmetry from the eclipsed to the staggered arrangement allows mixing of d orbitals (Scheme 4) in a way that also helps to minimize that antibonding character.

This is well seen by looking at the HOMO of $[(Ind)_2Ni]$ and the LUMO of $[(\eta^5\text{-Ind})_2Fe]$, shown in Fig. 4 (left and right, respectively), where the effect of the mixing is evident. It explains the energy difference between this preferred conformation and the eclipsed one.

This orbital is reminding of the orbital shown in Fig. 3 for the cations $[(\eta^3\text{-Ind})(CO)_2(NCMe)_3Mo]^+$ and appears to be the most important orbital in determining the behavior of indenyl ligands.

2.2. The conversion of η^5-indenyl into η^3-indenyl complexes

In the previous section, it was shown that in pairs of complexes related by an indenyl haptotropic shift, induced either by ligand addition or electrochemically, the indenyl ligands exhibited different conformations. This means that normally a rotation of the indenyl ligand around a metal–centroid bond must take place as the indenyl rearrangement proceeds, and therefore steric effects may be important.

Electrochemically induced $\eta^5 \rightarrow \eta^3$ shifts are easier to study, as only electrons and no ligands are added to the reagent molecule. In the metal–indenyl interaction, for the system $[(\eta^5\text{-Ind})CpMo(CO)_2]^{2+}$, the LUMO is derived from the indenyl $3\pi_s$ orbital (Scheme 2). The interaction between the $3\pi_s$ orbital of the indenyl and the

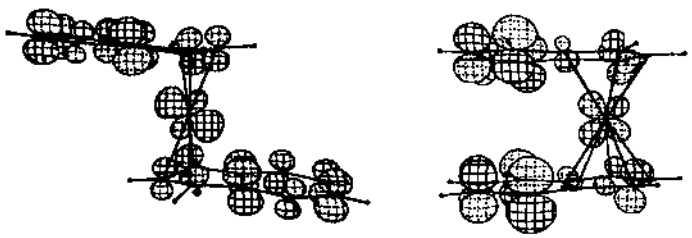

Fig. 4. The HOMO of $[(Ind)_2Ni]$ (left) and the LUMO of $[(\eta^5\text{-Ind})_2Fe]$ (right).

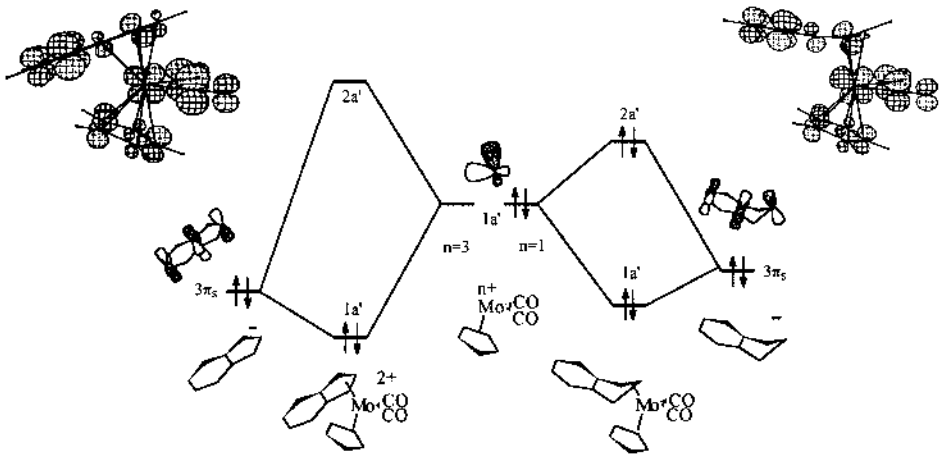

Fig. 5. Schematic diagram showing the relevant orbital in the interaction between $CpMoL_2^{3+,+}$ and one η^5-indenyl (left) or one η^3-indenyl (right).

corresponding orbital of the metal fragment is schematically shown in Fig. 5 (for η^5-indenyl on the left, and for η^3-indenyl on the right), and was drawn after EH calculations. This picture shows the effect of adding two electrons to $[(\eta^5\text{-Ind})CpMoL_2]^{2+}$ to form $[(\eta^3\text{-Ind})CpMoL_2]$ [4]. Notice that the η^5-indenyl ligand is taken in the same conformation as the η^3-indenyl one in order to keep some symmetry and have less mixing between orbitals.

The two extra electrons will occupy the metal–indenyl antibonding orbital, 2a′, shown in the left side. Folding the C5 ring leads to a strong stabilization of this orbital, as only three carbon atoms, rather than five, contribute to the metal–ligand repulsion (level 2a′, drawn in the right side). Some bonding molecular orbitals, arisen from interactions with other indenyl π orbitals, lose some bonding character, when only three carbon atoms, rather then five bind to the metal. This effect is responsible for a weaker bond of η^3-indenyl than η^5-indenyl to the metal.

The process taking place in the other situation, when an acetonitrile molecule approaches, for instance, $[(\eta^5\text{-Ind})(CO)_2(NCMe)_2Mo]^+$, and induces the $\eta^5 \rightarrow \eta^3$ rearrangement to form $[(\eta^3\text{-Ind})(CO)_2(NCMe)_3Mo]^+$ can be similarly described in terms of a molecular orbital picture [10]. Folding the indenyl stabilizes the orbital which is occupied by the two extra electrons. What is puzzling in this reaction is that substitution of the nitrile in the parent compound by isonitrile, a ligand of similar bulkiness, prevented the reaction from taking place. There is no reason for this to happen in view of our qualitative argument. The answer lies in the energetics of the reaction, shown in Fig. 6, and calculated with dft methods.

As the reaction takes place via an associative mechanism (approach of the incoming NCMe molecule), it is never favored on entropic grounds, and a negative enthalpic contribution must exist to lead to a favorable change in the Gibbs energy. What can be seen in Fig. 6 is that, according to dft calculations, ΔH is positive for the CNH derivative and negative for the nitrile.

This last result suggests that there are very subtle balances between different effects and modifying the system only slightly can lead to an unexpected reactivity. Another interesting conclusion from the dft calculations of the study of NCH dissociation from $[(\eta^3\text{-Ind})(CO)_2(NCMe)_3Mo]^+$ was the fact that the indenyl was already bent at a Mo–N distance of 3.17 Å, with the possible mechanistic implications [10].

Before finishing the section, let us consider again the electrochemical reaction of $[(\eta^5\text{-Ind})CpMoL_2]^{2+}$ to form $[(\eta^3\text{-Ind})CpMoL_2]$ [4] and imagine what happens after addition of only one electron. Preliminary dft calculations on the paramagnetic cation ([4]b, d) indicate that the coordination geometry of the indenyl is qualitatively very similar to that described above for $[(Ind)_2Ni]$, both in the distribution of distances and the folding of the indenyl. Indeed, this cationic species has one extra electron in one indenyl, while $[(Ind)_2Ni]$ has two extra electrons for two indenyl groups.

2.3. How different is indenyl from cyclopentadienyl?

Many of the theoretical studies performed on indenyl complexes had as driving forces the wish to understand the indenyl effect [13,14]. In the η^5 coordination mode, the Cp binds a metal center more strongly than an indenyl, as pointed out by Mealli et al. [14], and as came from our extended Hückel studies on the 2-electron reduction of the bent molybdenocene complexes $[(\eta^5\text{-Cp/Ind})CpMo(CO)_2]^{2+}$ (A), $[(\eta^3\text{-Cp/Ind})CpMo(CO)_2]$ (B) and $[(\eta^5\text{-Cp/Ind})CpMo(CO)]$ (C) [22]. The reduction of the dication species A can formally lead to the haptotropic shift of one the polyene rings bonded to the metal, as described above, to give B, or to the loss of one carbonyl, both rings remaining η^5 bonded (C).

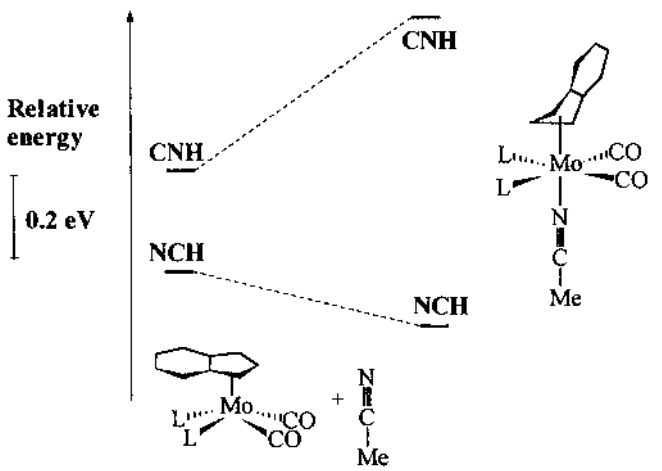

Fig. 6. Enthalpy change for the addition of NCH to $[(\eta^5\text{-Ind})(CO)_2L_2Mo]^+$, to form $[(\eta^3\text{-Ind})(CO)_2L_2(NCMe)Mo]^+$ (L = NCH, CNH).

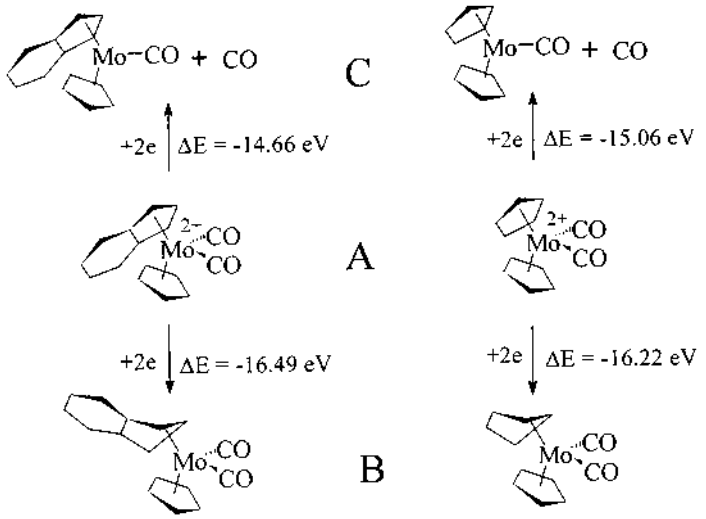

Scheme 5.

The dft calculations on the energetics of the changes from A to B, or C, are depicted in Scheme 5 and show an equivalence for the haptropic shift of both complexes (Cp and Ind). On the other hand, the species formed by carbonyl loss is clearly preferred in the bis-Cp system. We should stress that we are only calculating relative energies and no reaction pathways. Indeed, [(η^5-Ind)CpMo(CO)] has not yet been experimentally detected, [(η^3-Ind)CpMo(CO)$_2$] being always preferentially formed. In the bis-Cp system, both compounds have been characterized, though they do not interconvert directly [22].

EH overlap populations can help rationalizing this results. The η^5-Cp–Mo overlap population is 0.58, while the η^5-Ind–Mo overlap population is only 0.45, in complexes [(η^5-Cp/Ind)CpMo(CO)]. This is mainly due to the nodal features of the indenyl π orbitals when compared with the Cp ones, as discussed earlier (Scheme 2). In fact, in a Cp all the five carbon atoms contribute equaly to the bonding, while in the indenyl the two hinge carbon atoms (4 and 9) remain less involved in the M–C bonding. On the other hand, the bonding in a η^3 mode is stronger for an indenyl, as shown by the overlap populations calculated on [(η^3-Cp/Ind)CpMo(CO)$_2$] complexes (0.30 for the indenyl and 0.26 for the Cp). Therefore, the loss of symmetry following the folding of the C5 ring, breaking the degeneracy of the 1e orbitals, has a more dramatic effect on the Cp orbitals than on the indenyl ones. In an indenyl this asymmetry is already partially present in the planar ligand (Scheme 2).

We also analyzed the two related complexes [Mo(Ind)(NMe$_2$)$_3$] and [Mo(Cp)(NMe$_2$)$_3$], described in the literature [23], which are formally 14-electron species. However, each amide can donate four rather than two electrons, depending upon its orientation relative to the metal. Four electron donation is accomplished by simultaneous σ and π donations from the two nitrogen lone pairs and implies an

axial orientation of the amide substituents, in order to allow the π interaction between the $p_{\perp}$ nitrogen orbital and a metal d orbital parallel to the Cp or Ind ring plane (as the perpendicular ones are involved in the M–Cp/Ind bond). One might expect an 18-electron species, with an η^3-Cp/Ind and each of the amides donating four electrons. However, both EH on $[Mo(Ind)(NMe_2)_3]$ and dft calculations on $[Mo(Ind)(NH_2)_3]$ indicate that two of the amides are equatorially bonded and only the third has an axial orientation [24], the ring keeping a η^5 coordination. This means that we are in presence of a formally 16-electron complex, since only one of the amides donates four electrons. Dft calculations on the related $[Mo(Cp)(NMe_2)_3]$ ([23]b), produce a similar result, although the authors interpret a slight asymmetry in the bonding of the Cp ring as a η^3-Cp. We believe it is better described as a $(\eta^3 + \eta^2)$-Cp, given the small differences found in the M–C distances ($M-C_{1,2,3}$ 2.2–2.4 Å, and $M-C_{4,9}$ 2.5–2.7 Å). A similar pattern was also found with our dft calculations on $[Mo(Cp)(NH_2)_3]$, performed under different conditions [24].

3. Conclusions

The change in hapticity from (η^5-Ind)–M to (η^3-Ind)–M always seems to be induced by the occupation of a M–Ind π antibonding orbital originated by the interaction between the indenyl $3\pi_s$ and the appropriate metal d orbital (Scheme 6).

As a matter of fact, the loss of antibonding character of that orbital resulting from the increase of the M–C 4,5 distance, and the relatively low energy required for folding the indenyl are responsible for this behavior.

There is a significant difference between cyclopentadienyl and indenyl coordination to a metal center, arising mainly from the nodal properties of their π orbitals. η^5-Cp binds more strongly than η^5-Ind, and η^3-coordination is more favorable for the indenyl. The kinetics of the $\eta^5 \rightarrow \eta^3$ shift is also expected to be easier for the indenyl, since it requires that two carbon atoms, the ones more weakly bound, become non bonded. In spite of these constraints, $\eta^5 \rightarrow \eta^3$ shifts have been reported in Cp complexes, the final η^3-Cp complex being characterized in solution [25] or in the solid [26].

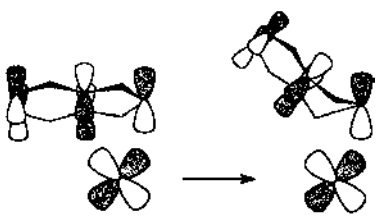

Scheme 6.

4. Models and calculational methods

The extended Hückel calculations [15] were done with the CACAO program [27] and modified H_{ij} values were used [28]. The basis set for the metal atoms consisted of ns, np and $(n-1)$d orbitals. The s and p orbitals were described by single Slater-type wave functions, and the d orbitals were taken as contracted linear combinations of two Slater-type wave functions. The parameters used for the metal atoms were the following (H_{ii} (eV), ζ). For Fe: 4s −9.17, 1.900; 4p −5.37, 1.900; 3d −12.70, 5.350, 1.800 (ζ_2), 0.5366 (C_1), 0.6678 (C_2). For Co; 4s −9.54, 2.000; 4p −4.51, 2.000; 3d −12.48, 5.550, 2.100 (ζ_2), 0.5680 (C_1), 0.6060 (C_2). For Ni: 4s −9.11, 1.825; 4p −5.15, 1.125; 3d −13.40, 5.750, 2.000 (ζ_2), 0.5683 (C_1), 0.6292 (C_2). For Mo: 5s −8.77, 1.960; 5p −5.60, 1.900; 4d −11.06, 4.542, 1.901 (ζ_2), 0.5899 (C_1), 0.5899 (C_2). Standard parameters were used for other atoms.

The calculations were performed with the real structures quoted along the text, as well as with models based on those structures and with idealised geometries and maximum symmetry, the results being qualitatively the same. The geometric details are given on the quoted references. For the [$(Ind)_2$M] complexes, the symmetry is C_{2v}, the conformation of the indenyl ligands is eclipsed and the indenyl ligands were taken as planar for M = Fe and Co. For M = Ni the η^3 coordination of the ligands was modelled by a 15° folding of the indenyl. The conformation of the two indenyl ligands in [$(Ind)_2$Ni] is staggered, the complex symmetry being C_{2h}. The bond distances (Å) were as follows: M–(C_5 ring centroid) 1.70, C–C 1.40, C–H 1.08.

Density functional calculations [16] were carried out on models based on the structures of the compounds described: $[(\eta^5\text{-Ind})MoL_2(CO)_2]^+$, $[(\eta^3\text{-Ind})Mo(NCH)_3(CO)_2]^+$, $[(\eta^5\text{-Ind})CpMoL_2]^{2+}$ and $[(\eta^3\text{-Ind})CpMoL_2]$, under C_s symmetry, using the ADF program [20] developed by Baerends and coworkers [29]. The slipping, folding and position of the indenyl and the positions of the other ligands were optimized. Vosko, Wilk and Nusair's local exchange correlation potential was used [30], with Becke's nonlocal exchange [31] and Perdew's correlation corrections [32]. The geometry optimization procedure was based on the method developed by Versluis and Ziegler [33], using the non-local correction terms in the calculation of the gradients. The core orbitals were frozen for Mo ([1–3]s, [1–3]p, 3d) and C, N, O (1s). Triple-ζ Slater-type orbitals (STO) were used for H 1s, C, N, O 2s and 2p, Mo 4s and 4p. A set of polarization functions was added: H (single ζ, 2p), C, N, O (single ζ, 3d).

Acknowledgements

We thank Carlos Romão, Isabel Gonçalves, and Carla Gamelas for the synthesis of most of the indenyl complexes mentioned in the text and for awakening our interest into trying to develop theoretical explanations and to predict new results, and also E. Herdtweck and V. Félix who determined the X-ray structures. Praxis XXI is acknowledged for partial funding of this research.

References

[1] M.E. Rerek, L.-N. Ji, F. Basolo, J. Chem. Soc. Chem. Commun. (1983) 1208.
[2] F.H. Allen, J.E. Davies, J.J. Galloy, O. Johnson, O. Kennard, C.F. Macrae, D.G. Watson, J. Chem. Inf. Comp. Sci. 31 (1991) 204.
[3] G.A. Miller, M.J. Therien, W.C. Trogler, J. Organomet. Chem. 383 (1990) 271.
[4] (a) J.R. Ascenso, C.G. Azevedo, I.S. Gonçalves, E. Herdtweck, D.S. Moreno, M. Pessanha, C.C. Romão, Organometallics 14 (1995) 3901. (b) M.J. Calhorda, V. Félix, C.A. Gamelas, I.S. Gonçalves, C.C. Romão, L.F. Veiros, in preparation. (c) M.J. Calhorda, C.A. Gamelas, I.S. Gonçalves, E. Herdtweck, J.P. Lopes, C.C. Romão, L.F. Veiros, XIIth FECHEM, Prague, Czech Republic, 1997. (d) M.J. Calhorda, V. Félix, C.A. Gamelas, I.S. Gonçalves, C.C. Romão, L.F. Veiros, XVII Reunión del Grupo Especializado de Química Organometálica, Barcelona, Spain, 1998.
[5] S. Lee, S.R. Lovelace, N.J. Cooper, Organometallics 14 (1995) 1974.
[6] C. Amatore, A. Ceccon, S. Santi, J.-N. Verpeaux, Chem. Eur. J. 3/2 (1997) 279.
[7] (a) R.M. Nielson, M.J. Weaver, Organometallics 8 (1989) 1636. (b) R.G. Finke, R.H. Voegeli, E.D. Laganis, V. Boekelheide, Organometallics 2 (1983) 347. (c) W.J. Bowyer, J.W. Merkert, W.E. Geiger, A.L. Rheingold, Organometallics 8 (1989) 191. (d) W.J. Bowyer, W.E. Geiger, J. Am. Chem. Soc. 107 (1985) 5657. (e) W.E. Geiger, Acc. Chem. Res. 28 (1995) 351.
[8] (a) L.-N. Ji, M.E.Rerek, F. Basolo, Organometallics 3 (1984) 740. (b) R.M. Kowalewski, A.L. Rheingold, W.C. Trogler, F. Basolo, J. Am. Chem. Soc. 108 (1986) 2460. (c) Z. Zhou, C. Jablonski, J. Brisdon, J. Organomet. Chem. 461 (1993) 215. (d) R.N. Biagioni, A.D. Luna, J.L. Murphy, J. Organomet. Chem. 476 (1994) 183. (e) D.A. Brown, N.J. Fitzpatrick, W.K. Glass, H.A. Ahmed, D. Cunningham, P. McArdle, J. Organomet. Chem. 455 (1993) 157. (f) K.A. Pevear, M.M. Banaszak Holl, G.B. Carpenter, A.L. Rieger, P.H. Rieger, D.A. Sweigart, Organometallics 14 (1995) 512. (g) J.M. O'Connor, C.P. Casey, Chem. Rev. 87 (1987) 307.
[9] C.E. Garrett, G.C. Fu, J. Org. Chem. 63 (1998) 1370.
[10] M.J. Calhorda, C.A. Gamelas, I.S. Gonçalves, E. Herdtweck, C.C. Romão, L.F. Veiros, Organometallics 17 (1998) 2597.
[11] J.W. Faller, R.H. Crabtree, A. Habib, Organometallics 4 (1985) 929.
[12] (a) J.W. Faller, C.-C. Chen, M.J. Mattina, A. Jakubowski, J. Organomet. Chem. 52 (1973) 361. (b) T.A. Huber, F. Bélanger-Gariépy, D. Zargarian, Organometallics 14 (1995) 4997. (c) T.A. Huber, M. Bayrakdarian, S. Dion, I. Dubuc, F. Bélanger-Gariépy, D. Zargarian, Organometallics 16 (1997) 5811. (d) R.H. Crabtree, C.P. Panell, Organometallics 3 (1984) 1727. (e) T.B. Marder, J.C. Calabrese, D.C. Roe, T.H. Tulip, Organometallics 6 (1987) 2012.
[13] (a) A.K. Kakkar, N.J. Taylor, J.C. Calabrese, W.A. Nugent, D.C. Roe, E.A. Connaway, T.B. Marder, J. Chem. Soc. Chem Commun. (1989) 990. (b) D. O'Hare, J.C. Green, T.B. Marder, S. Collins, G. Stringer, A.K. Kakkar, N. Kaltsoyannis, A. Kuhn, R. Lewis, C. Mehnert, P. Scott, M. Kurmoo, S. Pugh, Organometallics 11 (1992) 48. (c) N.S. Crossley, J.C. Green, A. Nagy, G. Stringer, J. Chem. Soc. Dalton Trans. (1989) 2139. (d) T.M. Frankcom, J.C. Green, A. Nagy, A.K. Kakkar, T.B. Marder, Organometallics 12 (1993) 3688.
[14] C. Bonifaci, A. Ceccon, S. Santi, C. Mealli, R. Zoellner, Inorg. Chim. Acta 240 (1995) 541.
[15] (a) R. Hoffmann, J. Chem. Phys. 39 (1963) 1397. (b) R. Hoffmann, W.N. Lipscomb, J. Chem. Phys. 36 (1962) 2179.
[16] R.G. Parr, W. Yang, Density Functional Theory of Atoms and Molecules, Oxford University Press, New York, 1989.
[17] S.A. Westcott, A.K. Kakkar, G. Stringer, N.J. Taylor, T.B. Marder, J. Organomet. Chem. 394 (1990) 777.
[18] D.M.P. Mingos, M.I. Forsyth, A.J. Welch, J. Chem. Soc. Dalton Trans. (1978) 1363.
[19] T. Le Husebo, C.M. Jensen, Organometallics 14 (1995) 1087.
[20] Amsterdam Density Functional (ADF) program, release 2.01; Vrije Universiteit, Amsterdam, The Netherlands, 1995.
[21] J.R. Ascenso, I.S. Gonçalves, E. Herdtweck, C.C. Romão, J. Organomet. Chem. 508 (1996) 169.

[22] M.J. Calhorda, C.A. Gamelas, C.C. Romão, L.F. Veiros, in preparation.
[23] (a) X. Yan, A.N. Chernega, N. Metzler, M.L.H. Green, Chem. Soc. Dalton Trans. (1997) 2091. (b) J.C. Green, R.P.G. Parkin, X. Yang, A. Haaland, W. Scherer, M. Tapifolsky, J. Chem. Soc. Dalton Trans. (1997) 3219.
[24] M.J. Calhorda, L.F. Veiros, unpublished results.
[25] W. Simanko, V.N. Sapunov, R. Schmid, K. Kirchner, S. Wherland, Organometallics 17 (1998) 2391.
[26] L.G. Bell, H.H. Brintzinger, J. Organomet. Chem. 135 (1977) 173.
[27] C. Mealli, D.M. Proserpio, J. Chem. Ed. 67 (1990) 39.
[28] J.H. Ammeter, H.-J. Bürgi, J.C. Thibeault, R. Hoffmann, Am. Chem. Soc. 100 (1978) 3686.
[29] (a) E.J. Baerends, D. Ellis, P. Ros, Chem. Phys. 2 (1973) 41. (b) E.J. Baerends, P. Ros, Int. J. Quantum Chem. S12 (1978) 169. (c) P.M. Boerrigter, G. te Velde, E.J. Baerends, Int. J. Quantum Chem. 33 (1988) 87. (d) G. te Velde, E.J. Baerends, J. Comp. Phys. 99 (1992) 84.
[30] S.H. Vosko, L. Wilk, M. Nusair, Can. J. Phys. 58 (1980) 1200.
[31] A.D. Becke, J. Chem. Phys. 88 (1987) 1053.
[32] (a) J.P. Perdew, Phys. Rev. B33 (1986) 8822. (b) J.P. Perdew, Phys. Rev. B34 (1986) 7406.
[33] (a) L. Versluis, T. Ziegler, J. Chem. Phys. 88 (1988) 322. (b) L. Fan, T. Ziegler, J. Chem. Phys. 95 (1991) 7401.